transformation of coordinate systems and vector components may be adopted.

Let us consider the rotation of the x- and y-axis about the origin to an angle β counterclockwise. Mathematically, we transform the (ρ, θ) coordinates to the (ρ^*, θ^*) coordinates, where

$$\begin{cases} \theta^* = \theta - \beta \\ \rho^* = \rho. \end{cases} \tag{A1}$$

Then the transformation of the field components can be obtained by

$$\begin{bmatrix} E_x^*(\rho^*, \theta^*) \\ E_y^*(\rho^*, \theta^*) \end{bmatrix} = \begin{bmatrix} \cos\beta & \sin\beta \\ -\sin\beta & \cos\beta \end{bmatrix} \begin{bmatrix} E_x(\rho, \theta) \\ E_y(\rho, \theta) \end{bmatrix}. \tag{A2}$$

Substituting (3) into (A2), we have

$$\begin{cases} E_x^* = A^* \cos[l\theta^* + (l \mp 1)\beta] \\ E_y^* = \pm A^* \sin[l\theta^* + (l \mp 1)\beta] \end{cases} \tag{A3}$$

with

$$A^* = \left(\sqrt{2}\,\frac{\rho^*}{w}\right)^l L_p^l\left(\frac{2\rho^{*2}}{w^2}\right)\frac{w_0}{w}\exp\left(-\frac{\rho^{*2}}{w^2}\right) \cdot \exp\left[-jkz + j(2p+l+1)\Phi - j\frac{k\rho^{*2}}{2R}\right]. \tag{A4}$$

Now, consider that the "series A" mode is rotated to $\beta = \pi/2(l-1)$, (A3) is reduced to

$$\begin{cases} E_x = -A\sin l\theta \\ E_y = A\cos l\theta. \end{cases} \tag{A5}$$

These expressions are true for $l > 1$. The superscript * is dropped from now on. On the other hand, consider that the "series B" mode is rotated to $\beta = \pi/2(l+1)$, (A3) is reduced to

$$\begin{cases} E_x = -A\sin l\theta \\ E_y = -A\cos l\theta. \end{cases} \tag{A6}$$

These expressions are true for $l \geqslant 1$. Combining (A5) and (A6), we find

$$\begin{cases} E_x = -2A\sin l\theta \\ E_y = 0 \end{cases} \tag{A7}$$

which is identical to (2), apart from a constant factor. It appears that these expressions are only true for $l > 1$ but, using (4) and (A6), it is obvious that (A7) is also true for the special case $l = 1$.

Acknowledgment

One of the authors (K. M. Luk) wishes to thank Dr. W. K. Chan for his encouragement and comments in preparing this paper.

References

[1] H. Kogelnik and T. Li, "Laser beams and resonators," *Proc. IEEE*, vol. 54, pp. 1312–1329, Oct. 1966.
[2] M. Lax, W. H. Louisell, and W. B. McKnight, "From Maxwell to paraxial wave optics," *Phys. Rev.*, vol. 11, pp. 1365–1370, Apr. 1975.
[3] P. K. Yu and K. M. Luk, "High-order azimuthal modes in the open resonator," *Electron. Lett.*, vol. 19, pp. 539–541, July 1983.
[4] C. W. Erickson, "High order modes in a spherical Fabry-Perot resonator," *IEEE Trans. Microwave Theory Tech.*, vol. MTT-23, pp. 218–223, Feb. 1975.
[5] C. W. Erickson, "Perturbation theory generalized to arbitrary (p, l) modes in a Fabry–Perot resonator," *IEEE Trans. Microwave Theory Tech.*, vol. MTT-25, p. 958, Nov. 1977.
[6] A. L. Cullen, "On the accuracy of the beam-wave theory of the open resonator," *IEEE Trans. Microwave Theory Tech.*, vol. MTT-24, pp. 534–535, Aug. 1976.
[7] G. Sansone, *Orthogonal Functions*. New York: Interscience, 1959, ch. IV.

Phased-Dipole Applicators for Torso Heating in Electromagnetic Hyperthermia

YONG-GANG GU AND OM P. GANDHI, FELLOW, IEEE

***Abstract*—The paper describes a two-dipole applicator that is capable of providing in-depth and relatively uniform rates of heating (SAR's) over the volume of the torso and greatly reduced SAR's for the rest of the body. Power coupling efficiencies in excess of 60 percent and fairly low leakage power densities have been measured for the applicator.**

I. Introduction

Hyperthermia is considered to be a potentiator of radiation therapy or chemotherapy for many forms of cancer [1],[2]. Among the various techniques, such as conventional heating, or heating by ultrasonic or electromagnetic energy, the latter offers the advantage of minimal reflections at interfaces with bones or with air cavities. Because of the somewhat shallower depth of penetration of electromagnetic energy (on the order of 5–10 cms), phased-array applicators have, however, had to be used to obtain in-depth heating at the tumor sites. In our previous work [3], we have proposed and provided theoretical designs of applicators consisting of short dipoles which may be altered in position and magnitude and phase of excitation for each of its elements so as to obtain minimum deviation from prescribed inhomogeneous rates of heating (SAR's) for the various parts of the body. Recognizing that designs for multidipole applicators for prescribed temperature distributions would be of greater interest, we have also recently started to develop an inhomogeneous thermal model of man to allow for inhomogeneities of tissue electrical and thermal properties and for increase in blood flow rates due to vasodilation at elevated temperatures [4]. This paper gives the experimental results obtained with scale models on phased-dipole applicators for torso heating. Given here are the efficiencies for whole-body coupling, the SAR distributions over the volume of the torso and elsewhere within the body, and the strength of the leakage fields from the cylindrical metal casing.

II. Phased-Dipole Applicators

A conceptual illustration of the multidipole applicator is shown in Fig. 1. The applicator uses short dipoles (of lengths less than or equal to 0.1 × wavelength) whose respective positions and excitations (magnitude and phase) are obtained on the basis of numerical calculations with a block model of man [5] for minimum deviation from prescribed inhomogeneous SAR's for the various parts of the body. A metal cylinder, which may, of course, be constructed of metal screening, helps to contain the fields to the absorber that is the human body. The radius of the cylinder is not critical but image theory must be used to correct for the cylinder in numerical calculations. Of the various designs presented in [3], the one used for the present experiments is the applicator design for abdominal heating. For this application, one dipole placed ventrally in the symmetrical plane at a radial distance of 0.35 m and at a location of 1.0 m above the base of the feet was found to be adequate to give SAR's in the abdominal volume that were three times or more than those for the rest of

Manuscript received August 5, 1983; revised January 23, 1984. This work was sponsored by the University of Utah Research Committee.
The authors are with the Department of Electrical Engineering, University of Utah, Salt Lake City, UT 84112.

0018-9480/84/0600-0645$01.00

TABLE I
COMPOSITIONS OF THE BIOLOGICAL-PHANTOM MIXTURES USED TO FILL THE FIGURINE CAVITIES [8]

Figurine Height cm	Experimental Frequency MHz	Simulated Frequency MHz	Percent Composition of the Biological-phantom Mixture					
			NaCl	H_2O	P.E.P.	S.S.	ϵ_1	$\sigma/\omega\epsilon_0$
40.6	370	86.0	2.02	75	12.98	10	57.0	110.3
33.0	370	69.8	2.2	75	12.8	10	57.0	136.1
40.6	450	104.5	2.06	75	12.44	10.5	47.5	99.37

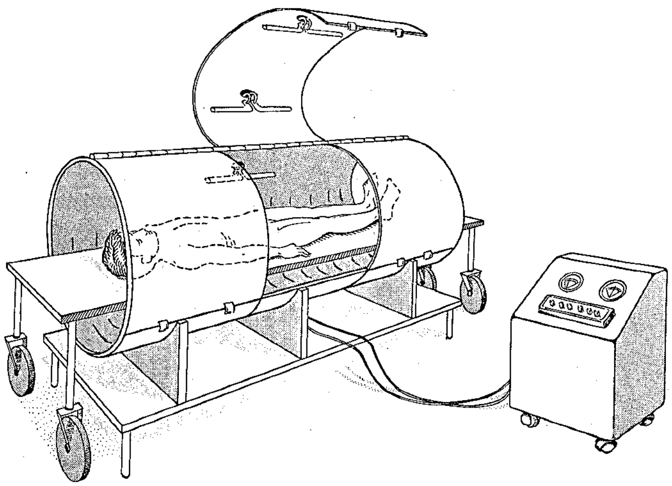

Fig. 1. A conceptual illustration of the multidipole applicator.

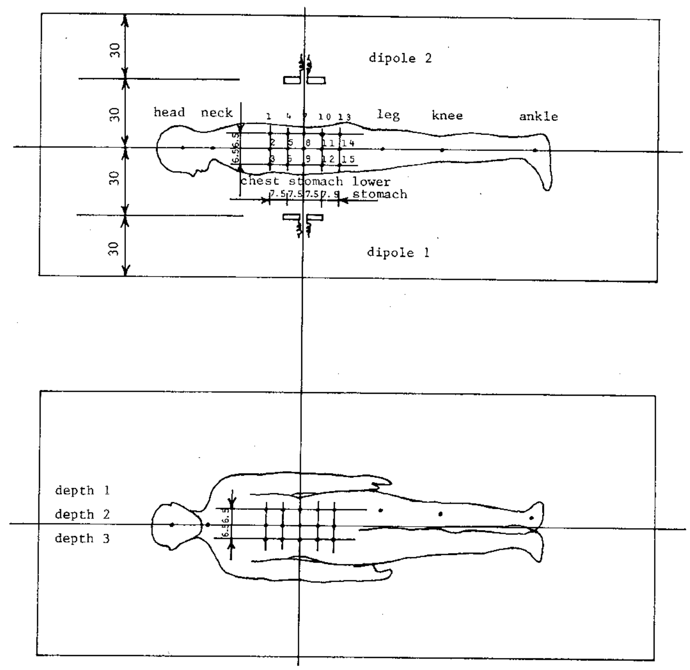

Fig. 2. The measurement points used for SAR distribution.

the body, i.e., for the head, the neck, the thigh, the knee, and the ankles.

The present experiments have been performed with 40.6- and 33.0-cm height man-shaped biological phantom-filled figurines placed concentrically inside an aluminum cylinder of diameter 28 cm and length 85 cm. Experiments have been performed at frequencies of 370 and 450 MHz at which 0.1-λ linear dipoles (rod diameter = 1.2 cm) fed with quarter-wavelength split-coax baluns [6] have been used as the irradiating elements. Feed-point impedance of a short dipole is known to be capacitive; two compensating lumped inductors (diameter 5 mm, about 4 turns) one for each of the two arms of the dipole are therefore used before these are connected to the balun. The inductance of these inductors and the stub lengths of a double stub tuner (Weinschel model DS-1096) are adjusted to obtain typically less than 2-percent power reflected back to the generator.

From electromagnetic field theory, a near-field arrangement reduced by a factor β in all dimensions may be used to obtain RF absorption characteristics of the full-scale system, provided the irradiation frequency is scaled up by a factor of β. It is necessary, however, that the complex permittivity ($\epsilon_1 - j\sigma/\omega\epsilon_0$) used for the reduced-scale model correspond to the value at the lower frequency at which the actual SAR distribution is desired. With these scaling precautions, the SAR distribution is identical (although the magnitudes are higher by a factor of β) to that of the full-scale body. It should also be recognized that these values of SAR's would be obtained for an input that is β^2 times higher than that for reduced-scale experiments.

For the reduced-scale models, biological phantom mixtures of NaCl, H_2O, polyethylene powder (P.E.P.), and superstuff[1] (S.S.), given in Table I, have been used. The compositions are such as to obtain complex permittivities at the full-scale irradiation frequencies corresponding to those required to simulate the average properties of the tissues corresponding to 66.7-percent muscle, skin, and tissues with high water content and 33.3-percent fat, bone, and tissues with low water content [7].

The SAR's were calculated from the internal E-fields which were measured at various points (shown in Fig. 2) using a Narda model 26089 implantable probe. For each of the points in the torso, the E-fields were measured at depths of 2, 3.5, and 5 cm, respectively. The SAR's so calculated have been reduced by the scaling factor β to obtain the numbers for a full-scale model. These are given in Table II.

A second dipole placed in the central plane of symmetry diametrically opposite to the ventral dipole was used to obtain a more uniform in-depth SAR distribution than that possible with just a single dipole. Equal and in-phase power was provided to

[1]Obtained from Oil Research Center, Lafayette, La.

TABLE II
SAR'S IN W/KG CALCULATED FOR THE FULL-SCALE MODEL FOR AN IRRADIATED POWER OF 100 W. IRRADIATION FREQUENCY = 86.0 MHZ, COUPLING EFFICIENCY = 60.35 PERCENT, DISTANCE OF THE DIPOLE(S) FROM THE WALL(S) = 30 CM, DIAMETER OF THE CYLINDER = 1.2 M, WHOLE-BODY-AVERAGED SAR = 0.862 W/KG.

		One Radiating Dipole (Ventral)			Two Radiating Dipoles		
Anatomical Location	Meas. Point (Fig. 2)	8.6 cm Depth	15 cm Depth (Center of the Body)	21.5 cm Depth	8.6 cm Depth	15 cm Depth	21.5 cm Depth
Head			0.012			0.031	
Neck			0.052			0.044	
Chest	1	0.023	0.021	0.013	0.692	0.811	0.750
	2	0.253	0.235	0.171	0.686	0.758	0.700
	3	1.185	1.083	0.863	0.753	0.753	0.706
	4	0.078	0.046	0.026	0.692	1.194	1.278
	5	0.267	0.238	0.223	0.956	1.000	0.933
	6	1.392	1.153	1.025	0.921	0.941	0.755
Abdomen	7	0.078	0.061	0.041	0.875	1.077	0.953
	8	0.360	0.345	0.247	0.822	0.901	0.733
	9	1.556	1.481	1.202	0.877	0.938	0.825
	10	0.070	0.052	0.029	0.470	0.500	0.432
	11	0.403	0.384	0.264	0.545	0.592	0.476
	12	1.150	1.115	0.910	0.706	0.703	0.592
Lower Abdomen	13	0.041	0.026	0.021	0.276	0.293	0.258
	14	0.316	0.325	0.250	0.322	0.303	0.247
	15	0.851	0.735	0.641	0.421	0.412	0.322
Leg			0.203			0.197	
Knee			0.061			0.313	
Ankle			0.047			0.186	

The above values are based on averages of three readings for each of the locations. Standard deviation of these readings was typically within ±5 percent.

the dorsal dipole by means of a coaxial-T power splitter and equal lengths of the coaxial cables to the two dipoles. Also given in Table II are the whole-body-averaged SAR's and the efficiencies of electromagnetic coupling to the body for the various irradiation conditions. The whole-body coupling efficiencies were obtained by using a normal (0.9-percent) saline solution in the figurine cavity in place of the biological phantom mixtures and obtaining the averaged SAR from the increase in temperature as a result of 10–20 min of exposure [9]. Coupling efficiencies in excess of 60 percent are obtained.

For an input power of 5 W, fairly low leakage power densities on the order of 0.04–0.2 mW/cm^2 were measured in the planes just outside the cylinder at the two edges with the maximum power density measured at the center. A total power leakage is estimated to be on the order of 3 percent of the input power. Also, from scaling considerations, a maximum leakage power density on the order of $[0.2\times100/5\times(4.306)^2]=0.22$ mW/cm^2 is estimated for 100-W input to full-scale bodies.

Experiments were also performed with a 33.0-cm figurine at 372.5 MHz [full-scale irradiation frequency = 70.3 MHz] and with a 40.6-cm figurine at a higher frequency of 475 MHz [full-scale irradiation frequency = 110.3 MHz]. Results qualitatively similar to those given above were obtained with the two-sided exposure clearly superior to that of a single dipole. It is interesting that, as anticipated by numerical calculations, the SAR's in the nontorso regions of the body were fairly low with reasonably low values for the important head and neck regions.

III. CONCLUSIONS

In conclusion, we have presented the experimental results on a two-dipole applicator that is capable of depositing fairly deep and uniform SAR's throughout the torso with relatively low SAR's for the rest of the body. The applicator has a reasonable coupling efficiency of 61 percent, and the leakage power densities are fairly low. With improved numerical procedures, including the development of an inhomogeneous thermal model of man and the fast-Fourier-transform procedure for a finer inhomogeneous modeling of the body for SAR calculations, it may become possible to design multidipole applicators for physician-prescribed SAR or temperature distributions for the various parts of the body.

REFERENCES

[1] J. G Short and P F. Turner, "Physical hyperthermia and cancer therapy," *Proc. IEEE*, vol. 68, pp. 133–142, 1980.

[2] R. K. Jain and P. M. Gullino, "Thermal characteristics of tumors: Applications in detection and treatment," *Ann. N.Y. Acad. Sci.*, vol. 335, 1980.

[3] P. F. Wahid, M. J. Hagmann, and O. P. Gandhi, "Multidipole applicators for regional and whole-body hyperthermia," *Proc. IEEE*, vol. 70, pp. 311-313, 1982.

[4] I. Chatterjee and O. P. Gandhi, "An inhomogeneous thermal block model of man for the electromagnetic environment," *IEEE Trans Biomed. Eng*, vol. BME-30, pp. 707–715, Nov. 1983.

[5] M. J. Hagmann, O. P. Gandhi, and C. H. Durney, "Numerical calculation of electromagnetic energy deposition for a realistic model of man," *IEEE Trans. Microwave Theory Tech.*, vol. MTT-27, pp. 804–809, 1979.

[6] H. Jasik, *Antenna Engineering Handbook*. New York: McGraw-Hill, 1961.

[7] C. C. Johnson and A. W. Guy, "Nonionizing electromagnetic wave effects—Biological materials and systems," *Proc. IEEE*, vol. 60, pp. 692–718, 1972.

[8] O. P. Gandhi and K. Sedigh, "Biological phantom materials for simulating man at different frequencies," presented at the 1976 USNC/URSI Meet., Amherst, MA.

[9] O. P Gandhi, E. L. Hunt, and J. A. D'Andrea, "Deposition of electromagnetic energy in animals and in models of man with and without grounding and reflector effects," *Radio Sci.*, vol. 12, no. 6(S) pp. 39–47, Nov/Dec 1977.

[10] D. Borup and O. P. Gandhi, "Fast-Fourier-transform approach for calculation of SAR distributions for finely-discretized models of inhomogeneous lossy bodies," *IEEE Trans. Microwave Theory Tech.*, vol. MTT-32, pp. 355–359, Apr. 1984.